



UNIVERSIDADE D
COIMBRA

FACULDADE
DE CIÊNCIAS
E TECNOLOGIA

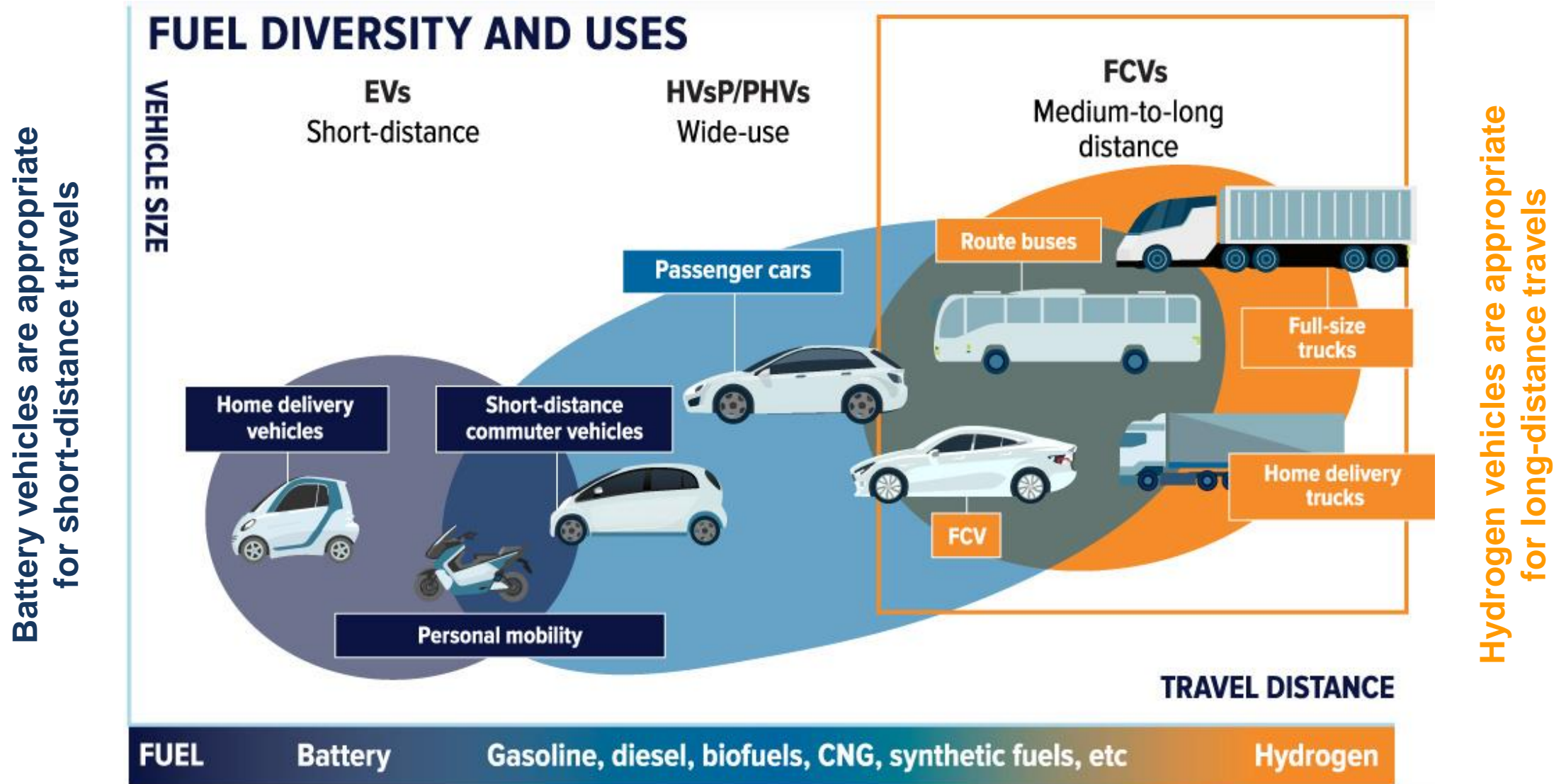
THE ROLE OF VISCOELASTICITY IN THE MECHANICAL MODELLING OF RUBBERS

C.M. Andrade¹ • J.R Barros¹ • D.M. Neto¹ • A. Ramalho¹ • M.C. Oliveira¹ • L.F. Menezes¹ • J.L. Alves²

¹CEMMPRE, Department of Mechanical Engineering, University of Coimbra, Portugal

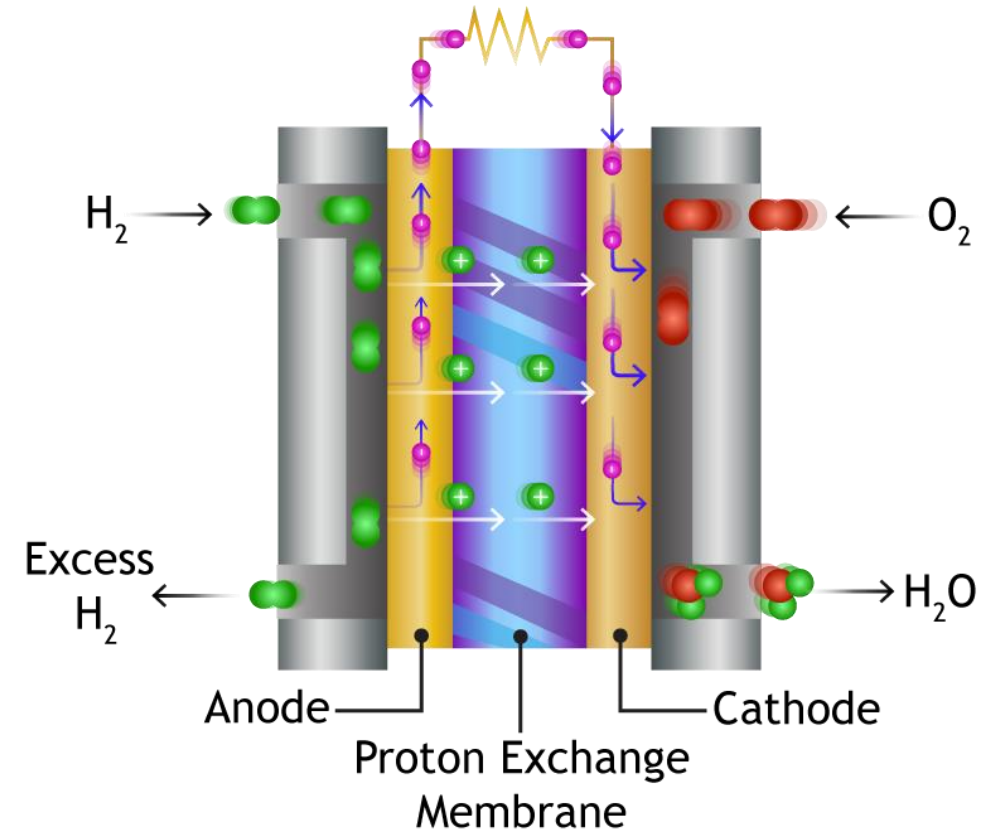
²CMEMS, Department of Mechanical Engineering, University of Minho, Portugal

Vehicles utilization according with the type of fuel



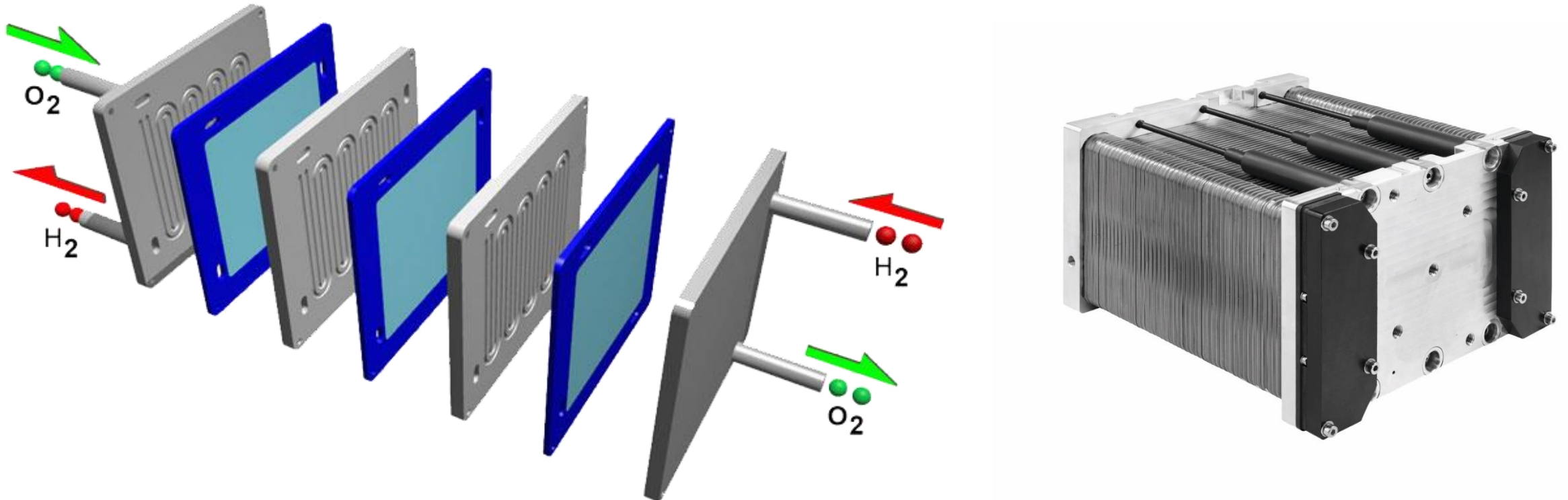
Hydrogen Electric Vehicles

- **Proton exchange membrane (PEM) fuel cells** are electrochemical devices that convert the chemical energy of a fuel (hydrogen) directly to electrical energy
- **Bipolar plates** are one of the main components of the PEM fuel cells, contributing to about 60–80% of the stack **weight** and 25–45% of the stack **cost**



PEM Fuel Cells

- Fuel cell is comprised of a series arrangement of “**repeating cell units**” stacked together
- A PEM fuel cell for a typical **passenger car** contains about **400–500 bipolar plates**



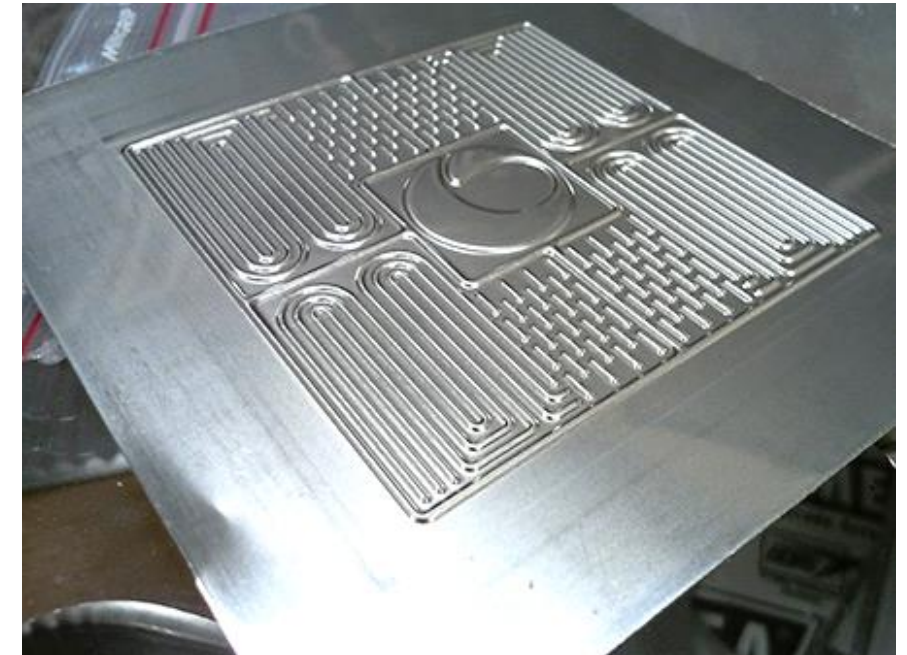
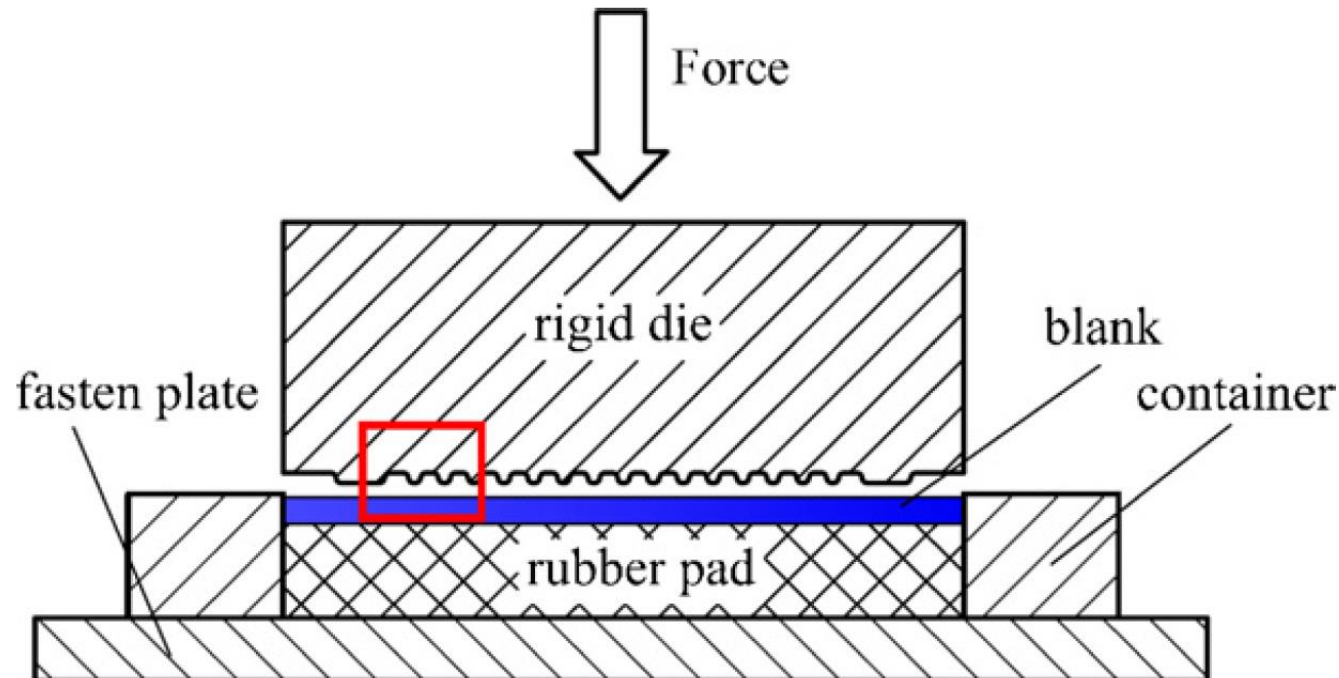
Bipolar plates

- Bipolar plate materials are broadly divided into **metallic** (e.g. titanium, stainless steel, aluminum) and **carbon-based** (e.g. graphite)
- Several manufacturing techniques are used to produce metallic bipolar plates (forming, milling and casting)
- **The rubber pad forming process** is adopted in the manufacturing of **thin stamped bipolar plates**



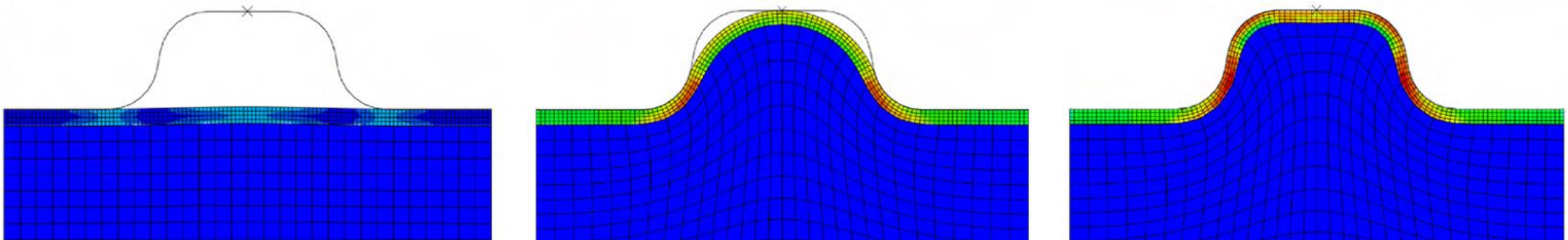
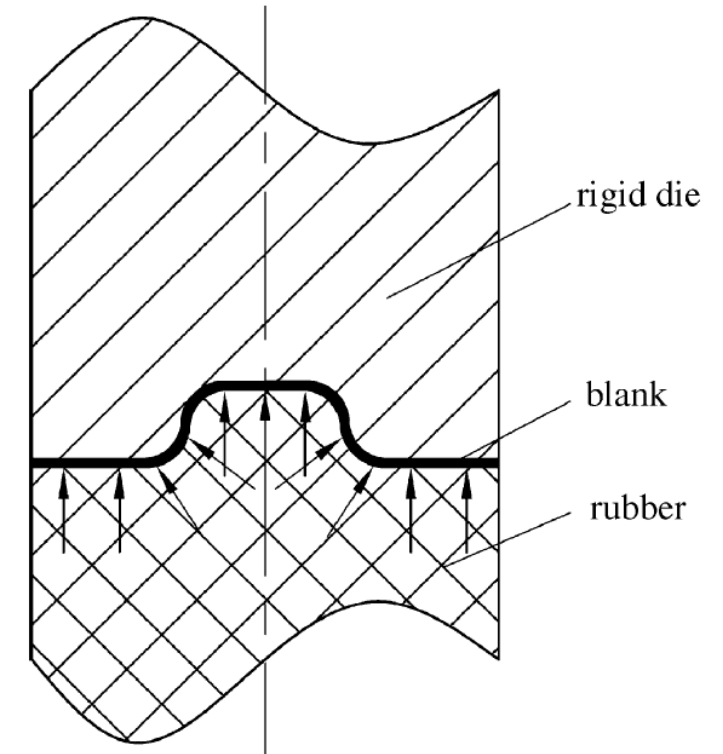
Stamped bipolar plates by rubber pad forming

- The main advantages are **low tooling costs**, **mark-free surface** of the workpiece and better formability when compared to conventional press technology
- The **wear of the rubber** is an issue in large quantity manufacturing



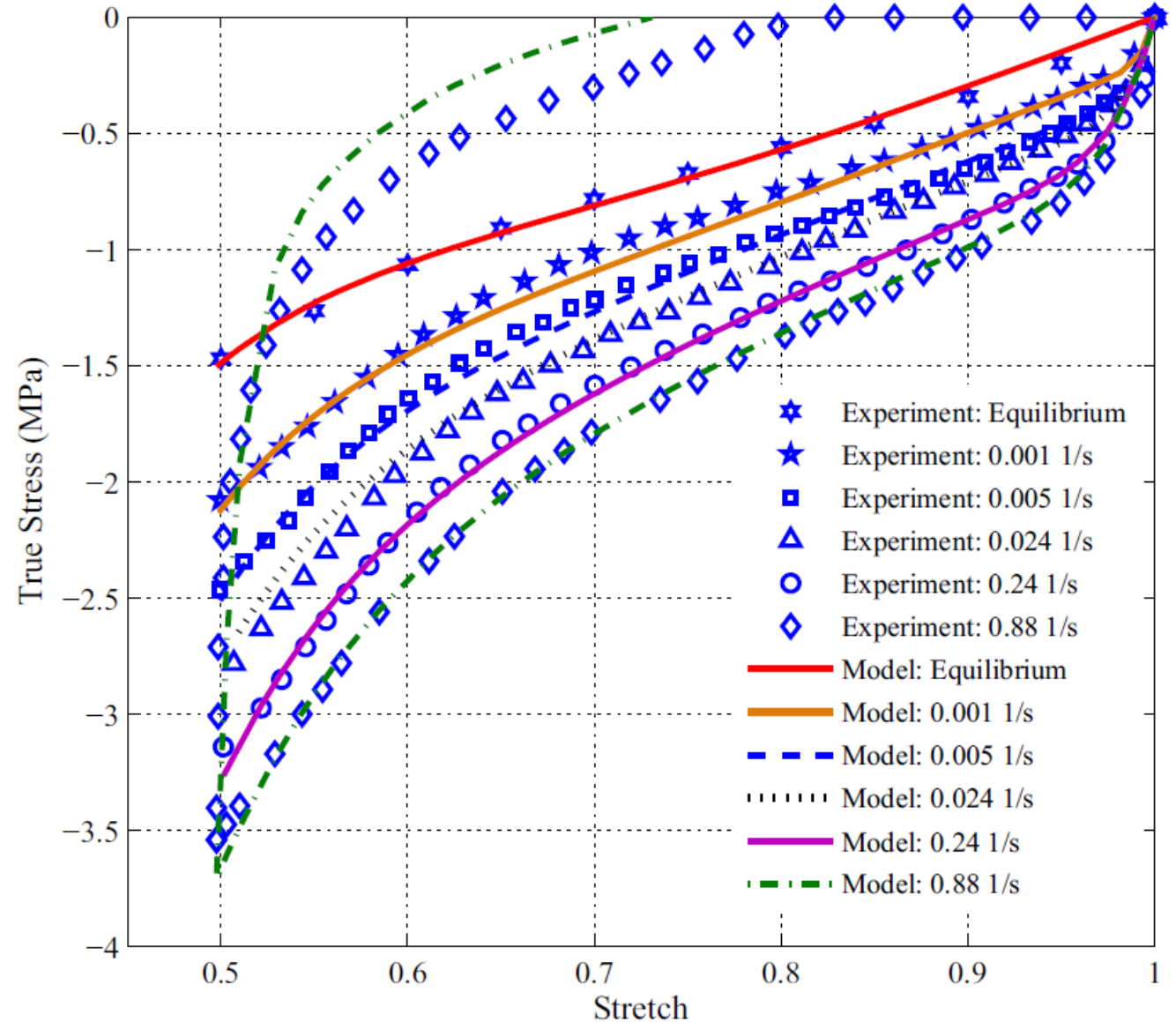
Numerical simulation of the rubber forming process

- **Numerical simulation** tools are adopted in the design and optimization of the forming processes to reduce **development cost** and **time-to-market** for new bipolar plates
- The accuracy of the numerical solutions is strongly dependent on the numerical models (**constitutive laws** for the blank and for the rubber pad) adopted in the finite element simulation



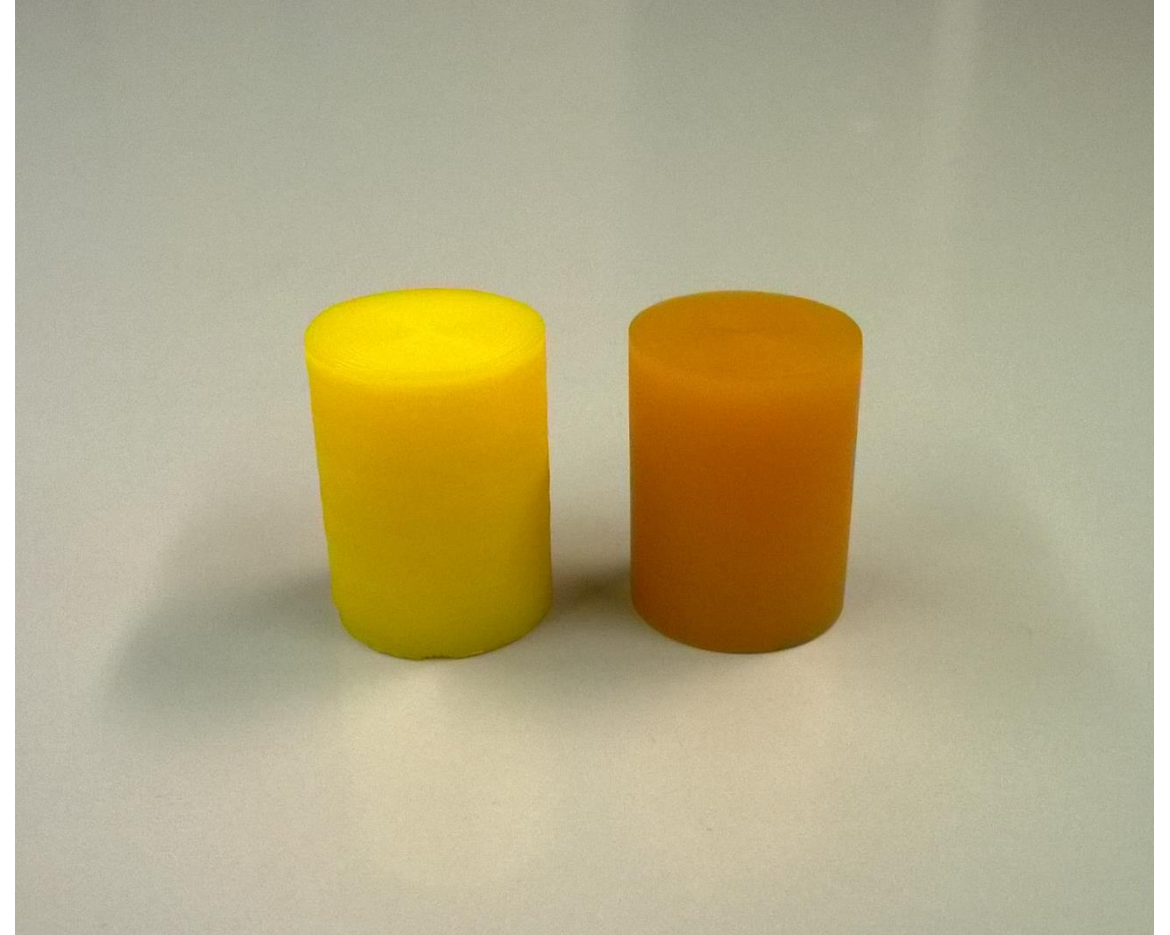
Visco-hyperelastic constitutive model

- The **rate-dependent** behavior of the rubber pad at **large deformations** is modelled by a **visco-hyperelastic constitutive model**
- The main objective of this study is to evaluate the **importance of the viscous effect** on the global behavior of the rubber pad during the forming process



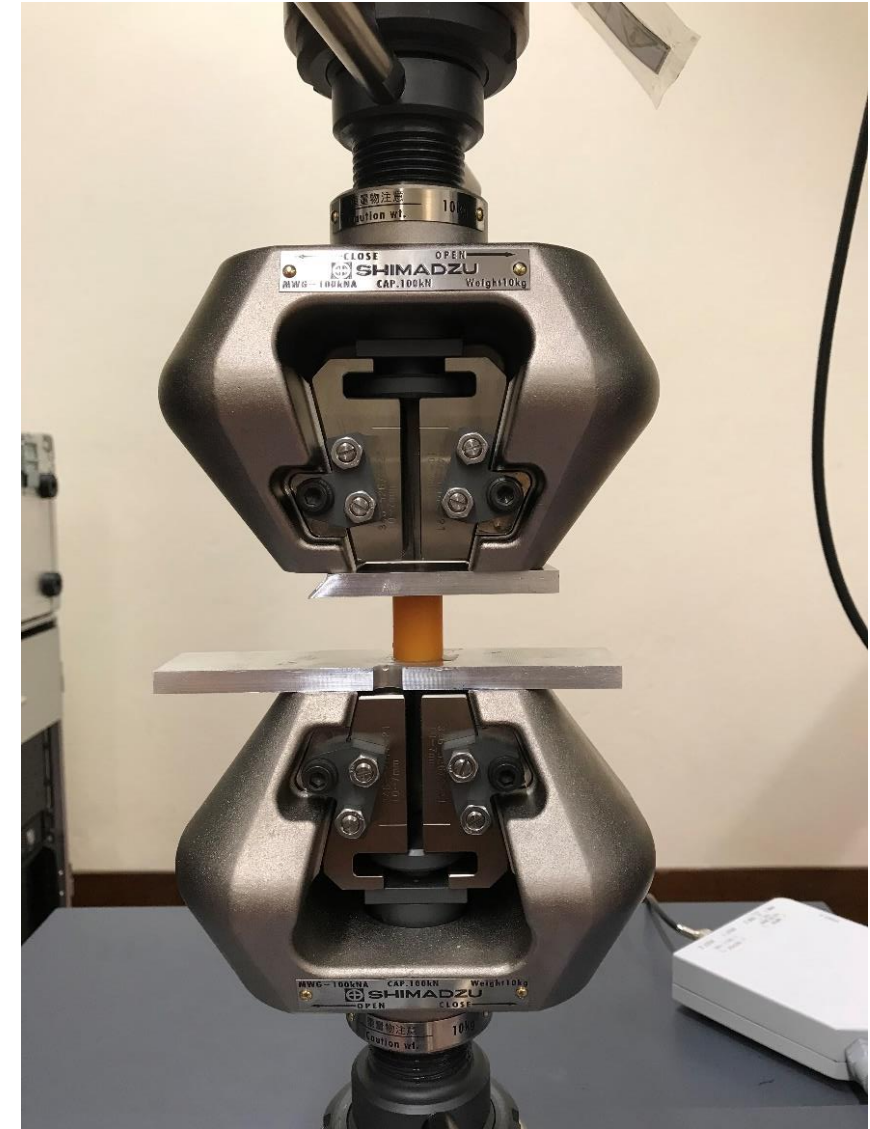
Rubber materials studied

- 2 different **polyurethane (PUR)** rubbers with different values of hardness:
 - ❑ **70 Shore A** (yellow specimen)
 - ❑ **95 Shore A** (orange specimen)
- Cylindrical specimens with 18 mm of diameter and 25 mm of height



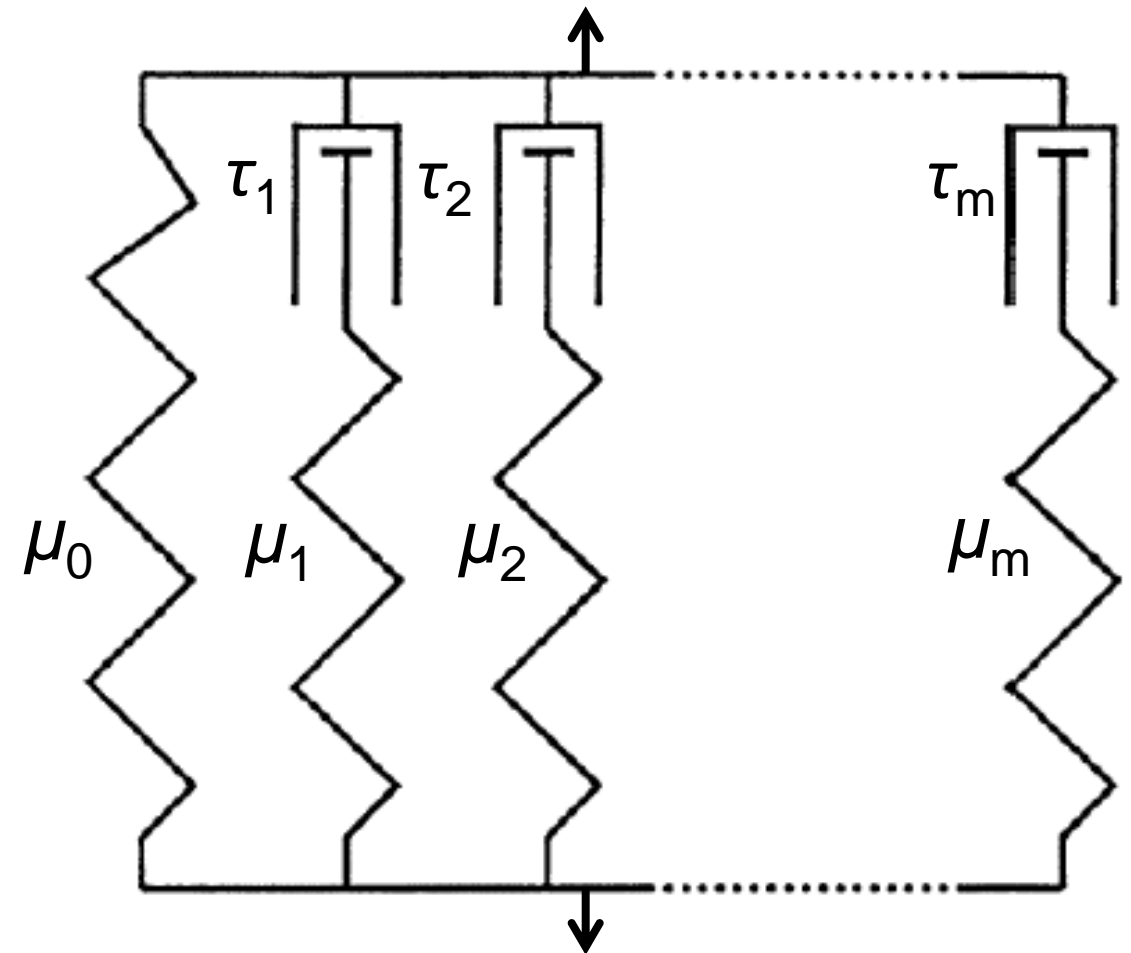
Mechanical tests performed

- **Uniaxial compression tests** comprising loading, permanency and unloading
 - ❑ 3 values of **grip speed** during the loading-unloading stage (0.05 mm/s, 0.5 mm/s and 5 mm/s)
- **Stress relaxation tests**
 - ❑ A stretch of 0.65 is kept constant for 10.000 seconds
 - ❑ Loading stage performed with the largest grip velocity (5 mm/s)



Visco-hyperelastic constitutive model

- The **hyperelasticity** is described by the Mooney-Rivlin model (2 parameters in the strain energy density function)
- The **viscoelasticity** is described by m Maxwell elements
- Each Maxwell element is defined by 2 parameters:
 - ❑ Relaxation time (τ)
 - ❑ $ak_i = \frac{\mu_i}{\mu_0}$

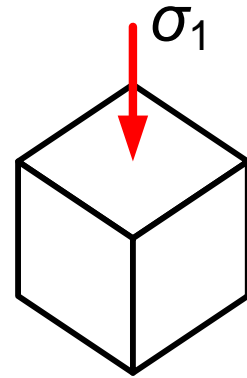


Rheological spring-dashpot model

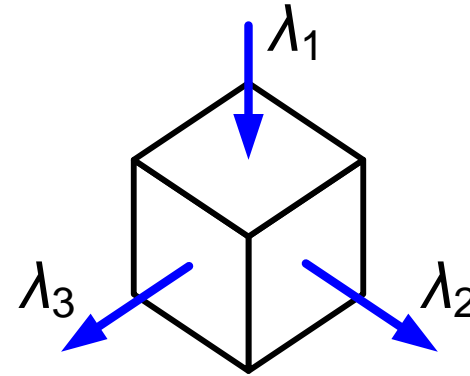
Uniaxial compression stress state

- Assumptions:

- Incompressible material
- Isotropic material



Stress



Strain

$$\begin{cases} \lambda_1 = \lambda \\ \lambda_2 = 1/\sqrt{\lambda} \\ \lambda_3 = 1/\sqrt{\lambda} \end{cases}$$

- 2nd Piola-Kirchhoff stress from hyperelasticity:

$$P_{MR} = 2(\lambda^{-1} - \lambda^{-4})(C_{10}\lambda + C_{01})$$

- 2nd Piola-Kirchhoff stress from viscoelasticity:

$$P_{MW_i}^{n+1} = \exp\left(-\frac{\Delta t}{\tau_i}\right) P_{MW_i}^n + \frac{ak_i\tau_i}{\Delta t} \left[1 - \exp\left(-\frac{\Delta t}{\tau_i}\right)\right] (P_{MR}^{n+1} - P_{MR}^n)$$

$$P_{Total} = P_{MR} + \sum_{i=1}^m P_{MW_i}$$

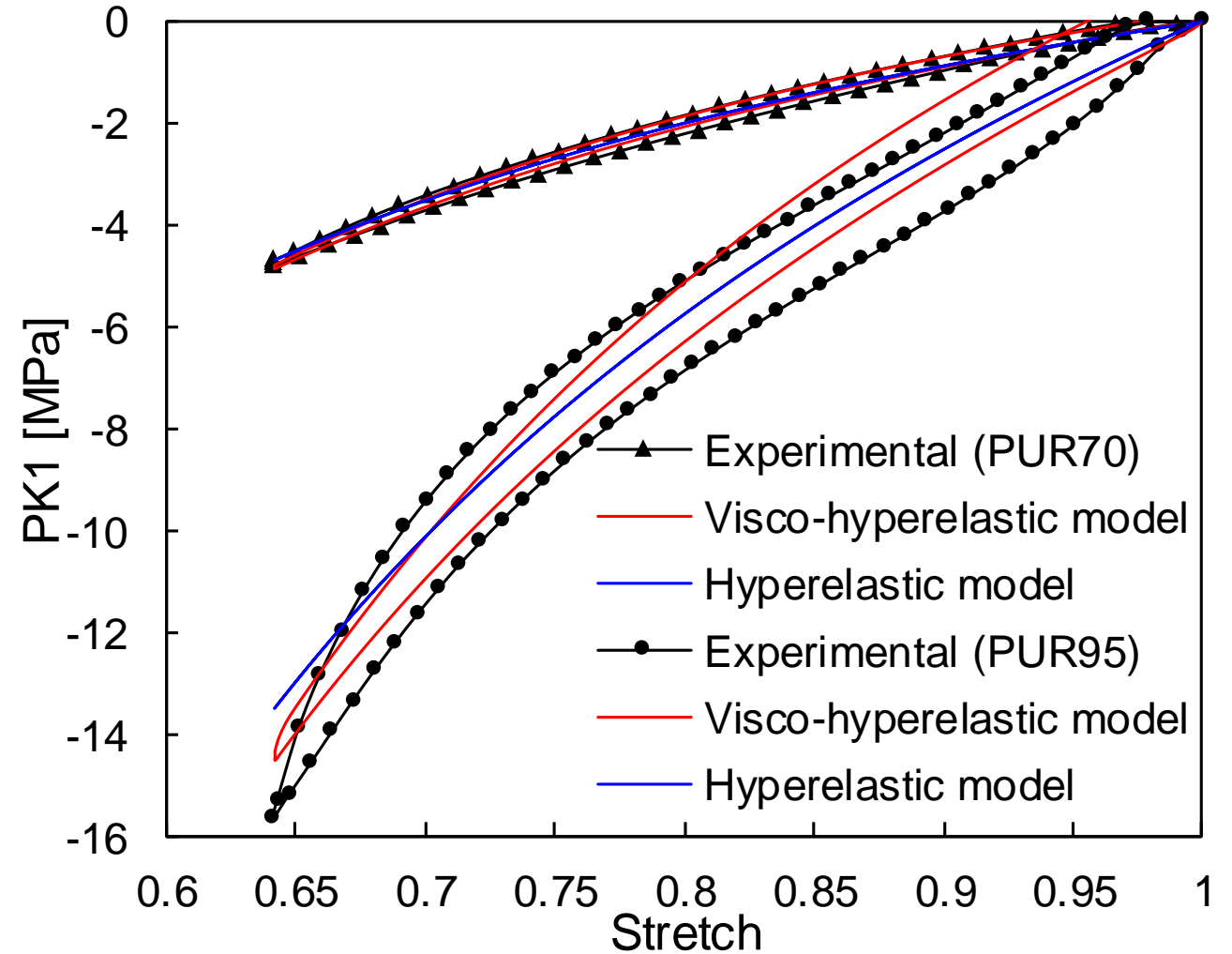
Least Squares fitting

- Minimization of the difference between numerical and experimental stress, considering **all tests simultaneously** (3 uniaxial compression tests + 1 stress relaxation test)
 - **Visco-hyperelastic model** (2+2x2=6 material parameters)
 - **Hyperelastic model** (2 material parameters)

	C_{10}	C_{01}	ak_1	ak_2	τ_1	τ_2
PUR70 visco-hyperelastic model	1.196	0.000	0.0956	0.0719	634.9	10.01
PUR70 hyperelastic model	1.317	0.000	-	-	-	-
PUR95 visco-hyperelastic model	3.485	0.000	0.1945	1.5170	19.25	0.090
PUR95 hyperelastic model	3.776	0.000	-	-	-	-

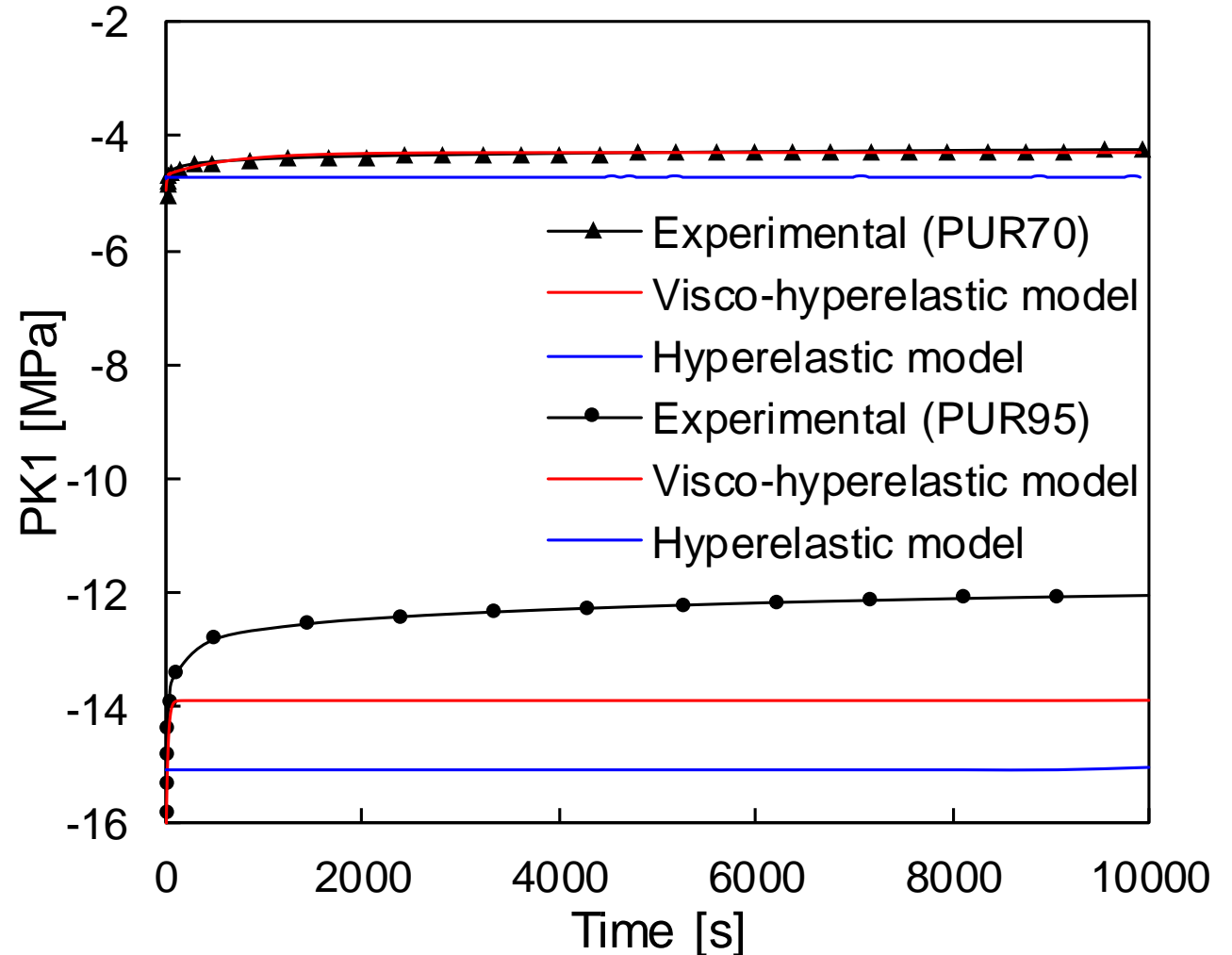
Uniaxial compression tests

- Loading and unloading at 0.5 mm/s grip speed
- Influence of the rubber hardness on the stress values
- The largest difference between loading and unloading curve occurs for the PUR95 (more pronounced viscous effect)



Stress relaxation tests

- Constant value of stretch = 0.65
- Improved prediction of the stress relaxation using the visco-hyperelastic constitutive model (PUR70)
- Regarding the PUR95, the experimental stress relaxation is underestimated by the numerical model (consequence of the relaxation time of each dashpot defining the Maxwell elements)



- Mechanical characterization of two polyurethane (PUR) rubbers
- The uniaxial loading/unloading shows that the viscous effect is more significant in the polyurethane with higher hardness value (PUR95)
- The adoption of the visco-hyperelastic model improves accuracy of the predicted stress
- Calibration of material parameters considers only the uniaxial stress state, but several strain paths arise in the rubber pad forming process

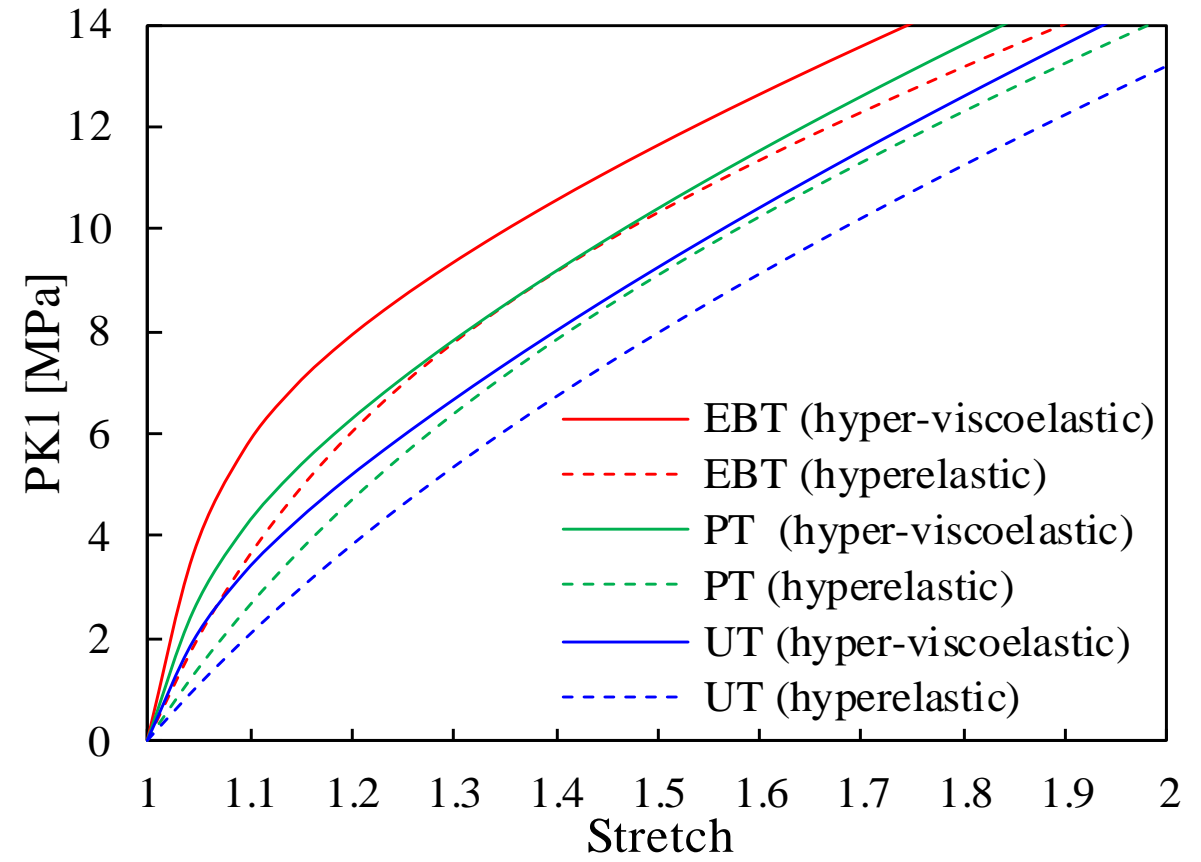
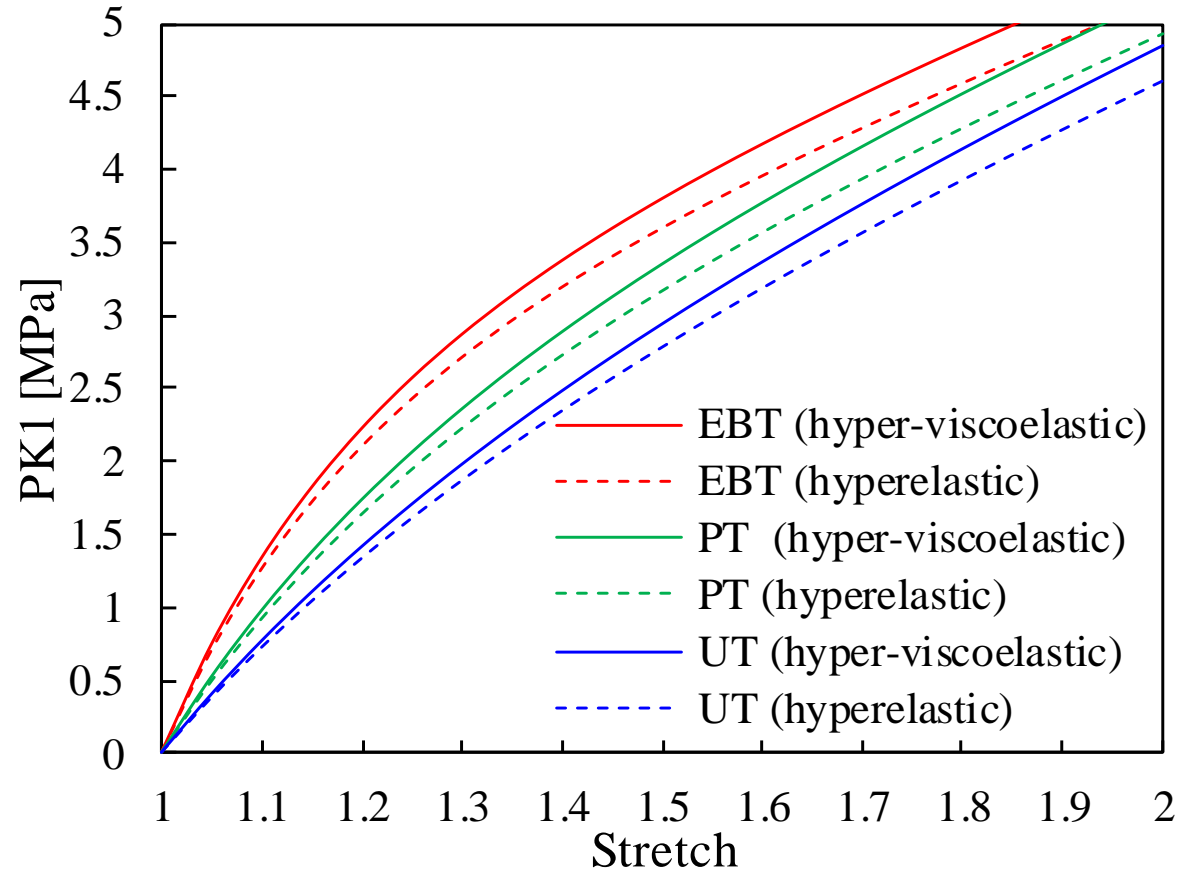
This research work was sponsored by national funds from the Portuguese Foundation for Science and Technology (FCT) under the projects with reference PTDC/EMS-TEC/0702/2014 (POCI-01-0145-FEDER-016779) and PTDC/EMS-TEC/6400/2014 (POCI-01-0145-FEDER-016876) by UE/FEDER through the program COMPETE 2020



Thank you for your attention!

Numerical prediction of stress evolution

- Uniaxial tension; Equi-biaxial tension; Planar tension

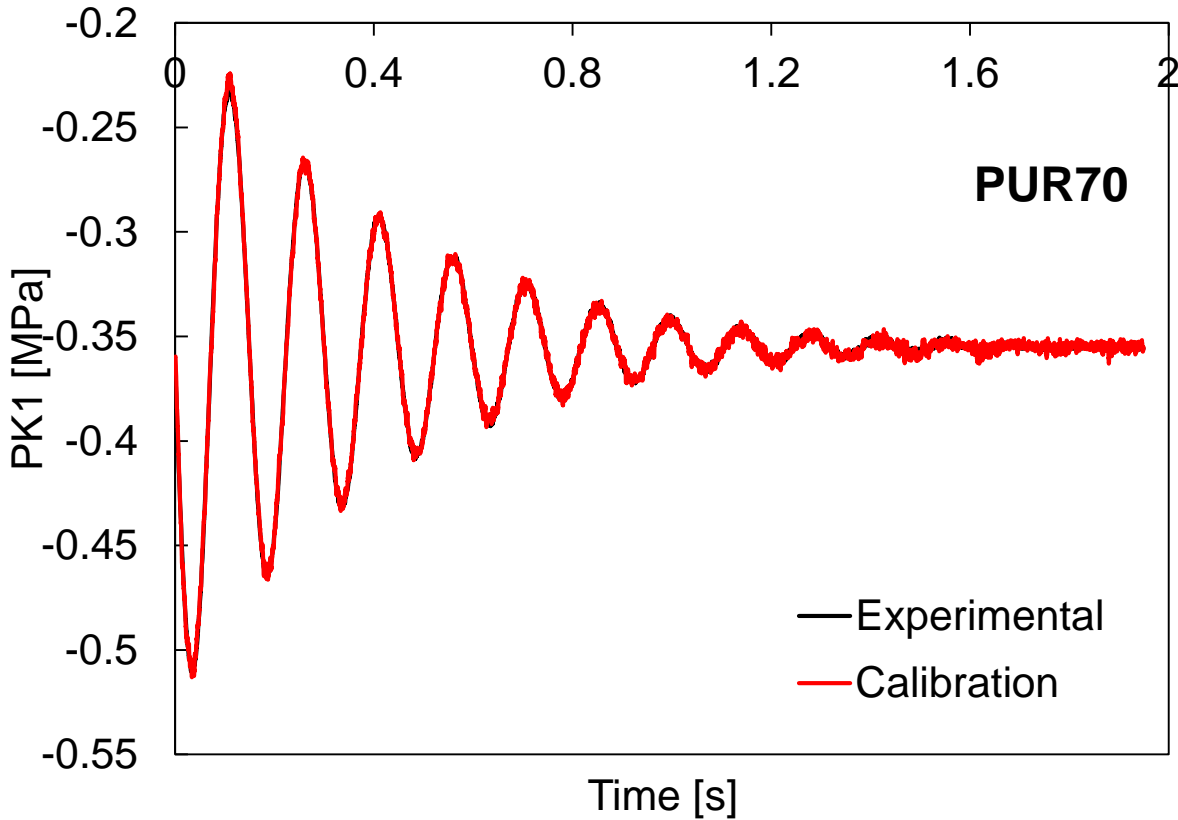


Yerzley's oscillograph

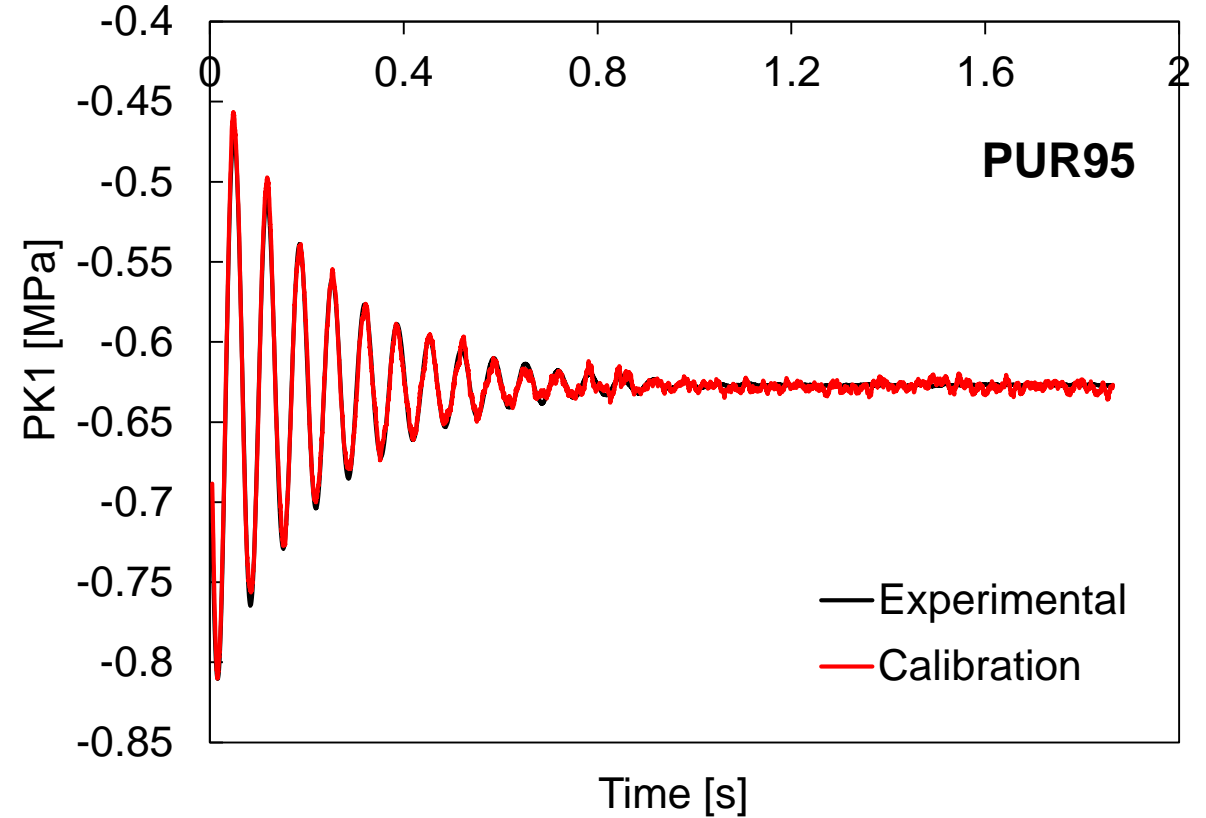
- A mass is placed on one arm of the beam at a distance L_m of the fulcrum
- The specimen is placed on the opposite side of the added mass at a distance L_p of the fulcrum
- The unbalanced arms of the beam produce a pre-compression force on the specimen
- An external perturbation applied to the beam makes the system oscillate
- Displacement and force values are recorded



Yerzley's oscillograph



C_{10}	C_{01}	ak_1	ak_2	T_1	T_2
0	1.1474	2.5024	0.1199	0.00198	1.25274



C_{10}	C_{01}	ak_1	ak_2	T_1	T_2
5.4882	0	0.4213	2.0021	482.665	0.00327